



## Results from the E-705 Electromagnetic Shower Position Detector \*

C. M. Jenkins<sup>10</sup>

M. Arenton<sup>11</sup>, T. Y. Chen<sup>9</sup>, S. Conetti<sup>6</sup>, B. Cox<sup>11</sup>, S. W. Delchamps<sup>4</sup>, B. Etemadi<sup>5</sup>,  
L. Fortney<sup>3</sup>, K. Guffey<sup>5</sup>, M. Haire<sup>6</sup>, P. Ioannu<sup>2</sup>, D.J. Judd<sup>8</sup>, C. Kourkouvelis<sup>2</sup>,  
I. Koutentakis<sup>2</sup>, J. Kuzminski<sup>6</sup>, K. W. Lai<sup>1</sup>, A. Manousakis-Katsikakis<sup>2</sup>, H. Mao<sup>9</sup>,  
A. Marchionni<sup>6</sup>, P.O. Mazur<sup>4</sup>, C.T. Murphy<sup>4</sup>, T. Pramantiotis<sup>2</sup>, R. Rameika<sup>4</sup>,  
L.K. Resvanis<sup>2</sup>, M. Rosati<sup>6</sup>, J. Rosen<sup>7</sup>, C.H. Shen<sup>9</sup>, Q. Shen<sup>3</sup>, A. Simard<sup>6</sup>,  
R. Smith<sup>4</sup>, L. Spiegel<sup>7</sup>, D. Stairs<sup>6</sup>, R. Tesarek<sup>3</sup>, W. Tucker<sup>5</sup>, T. Turkington<sup>3</sup>, F. Turkot<sup>4</sup>,  
L. Turnbull<sup>6</sup>, S. Tzamarias<sup>7</sup>, M. Vassiliou<sup>2</sup>, G. Voulgaris<sup>2</sup>, D.E. Wagoner<sup>8</sup>, C. Wang<sup>9</sup>,  
W. Yang<sup>4</sup>, N. Yao<sup>1</sup>, N. Zhang<sup>9</sup>, X. Zhang<sup>9</sup>, G. Zioulas<sup>6</sup>

1) University of Arizona, Tucson, Arizona 85721

2) University of Athens, Greece

3) Duke University, Durham, North Carolina 27706

4) Fermi National Accelerator Laboratory, Batavia, Illinois 60510

5) Florida A&M University, Tallahassee, Florida 32307

6) McGill University, Montreal, Quebec, Canada H3A 2TB

7) Northwestern University, Evanston, Illinois 60201

8) Prairie View A&M University, Prairie View, Texas 77445

9) Shandong University, Jinan, Shandong, People's Republic of China

10) University of South Alabama, Mobile, Alabama 36688

11) University of Virginia, Charlottesville, Virginia 22901

April 1989

\* Presented by C. M. Jenkins at the 1989 IEEE Nuclear Science Symposium, Orlando, Florida, November 9-11, 1988.



# Results from the E-705 Electromagnetic Shower Position Detector

C. M. Jenkins<sup>10</sup>

M. Arenton<sup>11</sup>, T. Y. Chen<sup>9</sup>, S. Conetti<sup>6</sup>, B. Cox<sup>11</sup>, S. Delchamps<sup>4</sup>, B. Etemadi<sup>5</sup>,  
L. Fortney<sup>3</sup>, K. Guffey<sup>5</sup>, M. Haire<sup>6</sup>, P. Ioannu<sup>2</sup>, D.J. Judd<sup>8</sup>, C. Kourkoulis<sup>2</sup>,  
I. Koutentakis<sup>2</sup>, J. Kuzminski<sup>6</sup>, K. W. Lai<sup>1</sup>, A. Manousakis-Katsikakis<sup>2</sup>, H. Mao<sup>9</sup>,  
A. Marchionni<sup>6</sup>, P. O. Mazur<sup>4</sup>, C. T. Murphy<sup>4</sup>, T. Pramantiotis<sup>2</sup>, R. Rameika<sup>4</sup>,  
L. K. Resvanis<sup>2</sup>, M. Rosati<sup>6</sup>, J. Rosen<sup>7</sup>, C. H. Shen<sup>9</sup>, Q. Shen<sup>3</sup>, A. Simard<sup>6</sup>,  
R. Smith<sup>4</sup>, L. Spiegel<sup>7</sup>, D. Stairs<sup>6</sup>, R. Tesarek<sup>3</sup>, W. Tucker<sup>5</sup>, T. Turkington<sup>3</sup>,  
F. Turkot<sup>4</sup>, L. Turnbull<sup>6</sup>, S. Tzamarias<sup>7</sup>, M. Vassiliou<sup>2</sup>, G. Voulgaris<sup>2</sup>, D.E. Wagoner<sup>8</sup>,  
C. Wang<sup>9</sup>, W. Yang<sup>4</sup>, N. Yao<sup>1</sup>, N. Zhang<sup>9</sup>, X. Zhang<sup>9</sup>, G. Zioulas<sup>6</sup>

- 1) University of Arizona, Tucson, Arizona
- 2) University of Athens, Athens, Greece
- 3) Duke University, Durham, North Carolina
- 4) Fermilab, Batavia, Illinois
- 5) Florida A&M University, Tallahassee, Florida
- 6) McGill University, Montreal, Quebec, Canada
- 7) Northwestern University, Evanston, Illinois
- 8) Prairie View A&M University, Prairie View, Texas
- 9) Shandong University, Jinan, Shandong, People's Republic of China
- 10) University of South Alabama, Mobile, Alabama
- 11) University of Virginia, Charlottesville, Virginia

## ABSTRACT

A fine grain hodoscope to measure the position of showers in the outer ( $|x| > 52\text{cm}$ ) region of the E-705 electromagnetic calorimeter is described. The hodoscope is constructed with two layers of vertical conducting plastic tubes for the X position measurement of showers. Y position measurement of showers was accomplished by cathode induced horizontal strips. A 50/50 argon, ethane bubbled through isopropyl alcohol at 0°C gas mixture was circulated through the tubes in parallel. The tubes were operated at +1.925 kv on the wire (below the region of saturated avalanche) in the limited proportionality mode. The hodoscope is described and results are presented for the position resolution, shower width, and charge detected as a function of calibration electron energy.

Fermilab experiment E-705<sup>1</sup> will study the hadronic production of charmonium and direct photon production. The experiment uses a 300 GeV/c  $\pi^+$ /p or a  $\pi^-/\bar{p}$  beam transported to a <sup>7</sup>Li target. The beam is capable of delivering an electron beam tunable between 2 and 100 GeV to calibrate the electromagnetic calorimeter. The spectrometer (Figure 1) includes a beam tagging system, charged particle tracking (upstream and downstream of a momentum analysis magnet), muon identification, and an electromagnetic calorimeter.

The electromagnetic calorimeter is 10m downstream of the target which detects photons from  $\chi \rightarrow J/\psi \gamma$  decay and direct photons. The main array is also part of the direct photon trigger.<sup>2</sup> The calorimeter (Figure 2) is divided into two parts, the converter and main array. The main array is 20.5 radiation lengths in depth and contains most of the shower energy for measurement. It is composed of an inner core of SCG1-C scintillating glass blocks<sup>3</sup> and SF5 Pb glass blocks on the outer regions. Upstream of the main array is the photon converter. The inner  $|X| \leq 52$  cm horizontal portion of the converter has a Pb radiator/gas calorimeter which also determines the photon position.<sup>4</sup> The outer  $|x| > 52$  cm region has an active converter made of columns of SCG1-C scintillating glass blocks 3.5 radiation lengths thick. The subject of this paper is a finely segmented shower position detector located downstream of the active converter and upstream of the main array blocks. The shower position detector consist of two panels 156 cm in X and 197 cm in Y with a 84 cm gap in the middle. Each panel has a 10 cm overlap with the central Pb/gas converter.

The shower position detector is constructed of vertical 10 mm by 7 mm (ID) conducting plastic tubes<sup>5</sup> (Figure 3a) with a wire centered in the tube (at positive high voltage). The anode wires are read out with LeCroy 2280 ADCs which provides the shower's X position. The wire was held on either end by a crimped copper capillary tube held in an end cap which sealed the end of the tube. A special compressed air powered crimper was used to crimp the wire in place. Two planes of tubes were epoxied between three planes of double sided copper clad G-10. The center board served as the ground plane for the tubes and the structural member in which the detector is suspended. A conducting epoxy made of powdered graphite mixed with amber Scotch 2216 structural adhesive was used to attach (electrically and structurally) the tubes to the ground plane. The outer G-10 boards had 8 mm strips cut on the copper surface adjacent to the tubes which are capacitively coupled to the anode and serve as the Y readout (Figure 3b). The Y strips were also readout by the LeCroy 2280 ADC. The detector used a gas mixture of 50/50 argon ethane bubbled through isopropyl alcohol at 0<sup>o</sup> C. The gas was distributed through holes drilled from the outside surface at the top end the the tubes (for gas feed) and at the bottom (for gas exhaust) A manifold covered the lines of holes on the top and bottom, upstream and downstream planes of tubes (Figure 3c).

The hodoscope constructed for the 1987 run was designed to be operated at a lower voltage than the previous model.<sup>6</sup> The operating voltage was low enough to require the signals to be amplified. The amplifiers used for the anode is shown in Figure 4a, and increased the charge collected by the ADC by a factor of 20 (the amplifiers drove a 50  $\Omega$  load). Figure 4b shows the cathode amplifier which inverts the cathode signal and amplified it by a factor of 75. A prototype of the detector (single layer of tubes with cathode strips) and amplifiers was tested with a <sup>106</sup>Ru source before the large detector was constructed. A small cylindrical section of the outer G-10 wall was removed to allow  $\beta$ s from the source to pass though the prototype and trigger two scintillator counters on the other side. The scintillators were in coincidence and triggered an ADC which digitized the charge collected for anode and cathode. The ADC was read out by an IBM personal computer that also histogrammed digitized charge of each event. The mean charge as a function of high voltage (reduced by the amplification) is shown in Figure 5.

Figure 6 shows the charge collected as a function of voltage for minimum ionizing muons in an earlier prototype<sup>6</sup> used in the 1985 data collection run of E-705. This detector used 50/50 argon-ethane bubbled through ethanol at 0°C but had identical wire size and tube dimensions. Two bands are present from the saturated avalanche and the limited streamer mode. The large detector was illuminated with a muon beam during the 1987 run to obtain the charge deposited per minimum ionizing particle. A value of  $0.45 \pm 0.03$  pc per minimum ionizing particle at 2100 volts was obtained and is superimposed onto Figure 6. No value was obtained for the cathode strips as the minimum ionizing signal for the anode was just above threshold.

The detector was exposed to the electron calibration beam to study its response as a function of energy. The electron beam was tagged and calibration events were recorded if there was only one electron indicated by the beam definition. These calibration events were studied in the hodoscope. For each calibration event, the peak block in the array was found and the hodoscope upstream of that block was investigated. The peak channel and the surrounding  $\pm 4$  channels in the hodoscope upstream of the peak block were used to study the shower. ADC distributions for these tubes were obtained for approximately 1000 showers, and the means and rms were obtained. These means and rms vs tube number in the shower were plotted in Figure 7 to show the profiles of the anode (X) and cathode induced (Y) projections for 6, 30, and 60 GeV electrons. Total ADC counts for an electron shower at a given energy were obtained by summing the ADC counts for the peak channels and  $\pm 4$  channels. The means and rms of distributions for the total ADC counts for 1000 showers at various energies were obtained and are plotted in Figure 8 for both the anode (X) and cathode induced (Y) projections.

Each individual shower in the interval of nine channels was also fitted to an exponential form:

$$e^{-|x-\mu|/\alpha}$$

where  $\mu$  is the mean position of the shower,  $\alpha$  corresponds to the shower width. The distribution of shower widths (resulting from the fit) was obtained for 1000 electron showers of a given energy. The mean and rms from this distribution were obtained and plotted in Figure 9 as a function of energy for both the anode (X) and cathode induced (Y) readout. Both the anode and cathode projections of the shower width appear to be flat as a function of shower energy with a mean value of  $\langle\alpha\rangle = 1.42 \pm 0.24$  cm for the anode and a value of  $\langle\alpha\rangle = 2.41 \pm 0.24$  cm for the cathode.

The position resolution for the hodoscope was obtained from the residuals of the shower position relative to the beam position. The table supporting the calorimeter was moved so that a given block was exposed to the electron beam tuned to a given energy. The beam position as measured by the beam tracking chambers was projected to the hodoscope. The peak tube in the cluster of tubes nearest the beam was used to select the center channel and the  $\pm 4$  channels for the fit to the exponential form. The fit to the shower was done to obtain the shower position ( $\mu$ ) and the residual to the beam ( $\mu$ -beam) was calculated for the shower. An overall offset for the table was subtracted from the residual to center it at zero. A distribution of the residuals for approximately 1000 electron showers was obtained. The rms of the residual distribution is the position resolution which includes the beam position error (due to multiple scattering and beam chamber resolution). The rms of the residual distribution was corrected for the beam position error by subtracting in quadrature the beam position error at each energy as estimated by monte carlo calculation. The resulting beam error corrected residual is the position resolution and it was obtained for all electron calibration energy and is shown in Figure 10 for the anode and cathode.

## **Acknowledgements**

The authors wish to thank the Fermilab technical staff for their help in the design and construction of this chamber, particular thanks go to Chuck Serritella and Denny Farnum. In addition, we wish to thank the Fermilab operating staff. The authors wish to acknowledge the U.S. Department of Energy, the Natural Sciences and Engineering Research Council of Canada, the Quebec Ministry of Education, and the Hellenic Science and Technology Agency for their support.

## Figure Captions

Figure 1. The E-705 spectrometer. The shower position detector is located in the electromagnetic calorimeter between the scintillation glass active converter and the main array 10 m downstream of the target.

Figure 2 a) The main array as viewed along the beam. The dotted line indicates the SF5, SCG1-C glass interface. The large blocks are 15 cm by 15 cm. There are 7.5 cm by 7.5 cm SCG1-C glass blocks close to the beam hole. b) A side view of the calorimeter with the active converter upstream and the main array downstream. The shower position hodoscope is between the active converter and the main array.

Figure 3 a) A cross sectional view of the top of the shower position detector. b) The cathode induced strips that were cut on the outer G-10 boards of the shower position detector and were adjacent to the plastic tubes. The strips compressed to 0.1 inch centered teeth suitable for a connector. c) Side view of the shower position detector that shows the gas port and the capillary tube used to hold the wire. No wires were lost due to slippage.

Figure 4 a) The anode amplifier used to multiply charge collected on the anode wire by 20. b) The cathode amplifier which inverts and amplifies by 75 the cathode induced signal.

Figure 5. Charge collected as a function of high voltage from  $\beta$  emitted from a  $^{106}\text{Ru}$  source for a small 20 cm by 30 cm test chamber. The charge collected is corrected for amplification.

Figure 6. Charge collected per minimum ionizing muons for a similar chamber (same tube dimensions and wire diameter) from a prototype of the 1985 E-705 shower position detector. The saturated avalanche mode and limited streamer mode are clearly visible and overlap. The charge collected from the anode of minimum ionizing muons for the present 1987 run chamber, corrected for amplification is superimposed.

Figure 7. Shower profiles of the anode and cathode readouts for various electron energies. a) 6 GeV, b) 30 GeV, c) 60 GeV. 30 GeV electron showers.

Figure 8. The total ADC counts for electron showers for a given energy was obtained from the mean of the distribution of total ADC counts for 1000 showers. The rms of the distributions are used as the error bars. The means are plotted as a function of energy. a) anode, b) cathode.

Figure 9. The width of individual showers was obtained from a fit to an exponential form. The mean from the distribution of the widths from 1000 showers, with the rms for error bars are plotted as a function of energy. The widths are reasonably flat with average values of  $\langle\alpha\rangle = 1.42 \pm 0.24$  cm for the anode and a value of  $\langle\alpha\rangle = 2.41 \pm 0.24$  cm for the cathode. a) Anode, b) cathode.

Figure 10. The residuals of the shower position (as determined from a fit of individual showers to an exponential form) minus the electron beam position were fitted to a Gaussian distribution. The sigma from the Gaussian fit with the error in the beam position due to multiple scattering subtracted in quadrature is plotted vs the reciprocal square root of the electron beam energy.

## References

- [1] M Binkley, *et al.*, Fermilab Proposal E-705 (1981).
- [2] G. Zioulas, *et al.*, IEEE Trans. Nucl. Sci., NS-36 (1989) 375.
- [3] D. E. Wagoner, *et al.*, Nucl. Inst. and Meth. **A238** (1985) 315; B. Cox, *et al.*, Nucl. Inst. and Meth. **A238** (1985) 321.
- [4] L. Spiegel, *et al.*, IEEE Trans. Nucl. Sci., NS-36 (1989) 86.
- [5] Tokyo Ink Co. 2-7-15 Tabata-Shinmachi, Kita-Ku Tokyo, Japan. Telex (265)5343.
- [6] C. M. Jenkins, *et al.*, E-705 Electromagnetic Shower Position Detector, Proceedings of the Gas Sampling Calorimetry Workshop II, October 31 and November 1 1985.

# FERMILAB HIGH INTENSITY LABORATORY SPECTROMETER

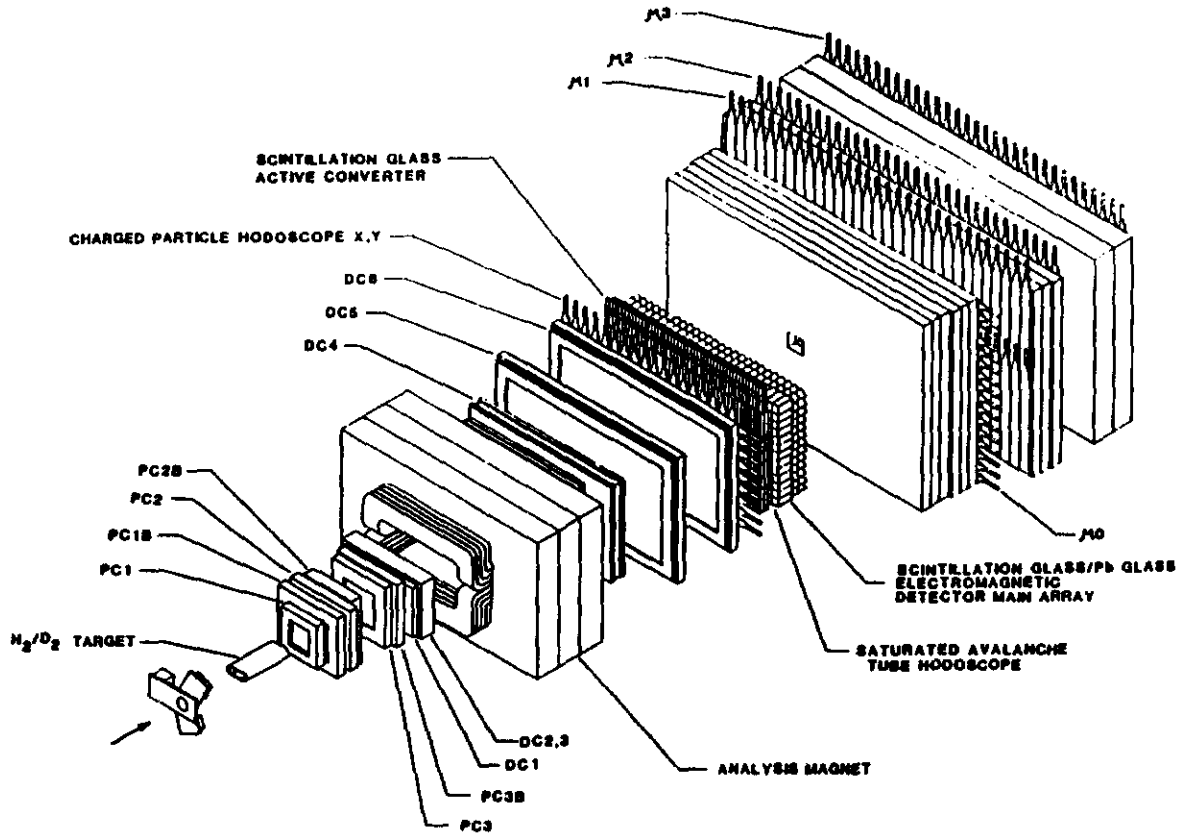
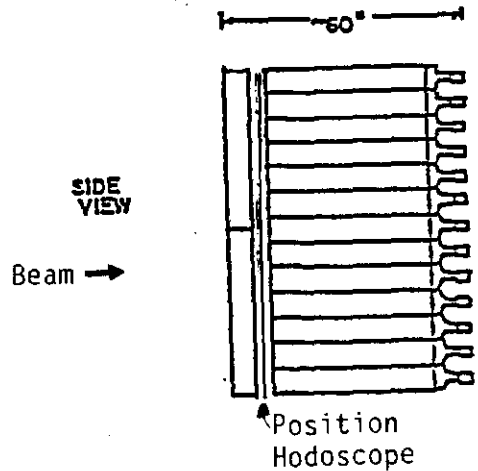


Figure 1

## E705 MAIN ARRAY - BLOCK NUMBERS

323	274	323	222	221	320	319	318	317	316	315	314	313	312	311	310	309	308	307	306	305	304	303	302	301
281	290	290	292	294	295	294	293	292	291	290	289	288	287	286	285	284	283	282	281	280	279	278	277	276
275	274	273	272	271	270	269	268	267	266	265	264	263	262	261	260	259	258	257	256	255	254	253	252	251
250	249	248	247	246	245	244	243	242	241	240	239	238	237	236	235	234	233	232	231	230	229	228	227	226
225	224	223	222	221	220	219	218	217	216	215	214	213	212	211	210	209	208	207	206	205	204	203	202	201
200	199	198	197	196	195	194	193	192	191	190	189	188	187	186	185	184	183	182	181	180	179	178	177	176
175	174	173	172	171	170	169	168	167	166	165	164	163	162	161	160	159	158	157	156	155	154	153	152	151
150	149	148	147	146	145	144	143	142	141	140	139	138	137	136	135	134	133	132	131	130	129	128	127	126
125	124	123	122	121	120	119	118	117	116	115	114	113	112	111	110	109	108	107	106	105	104	103	102	101
100	99	98	97	96	95	94	93	92	91	90	89	88	87	86	85	84	83	82	81	80	79	78	77	76
75	74	73	72	71	70	69	68	67	66	65	64	63	62	61	60	59	58	57	56	55	54	53	52	51
50	49	48	47	46	45	44	43	42	41	40	39	38	37	36	35	34	33	32	31	30	29	28	27	26
25	24	23	22	21	20	19	18	17	16	15	14	13	12	11	10	9	8	7	6	5	4	3	2	1

Beam View  
Figure 2A



Side View  
Figure 2B



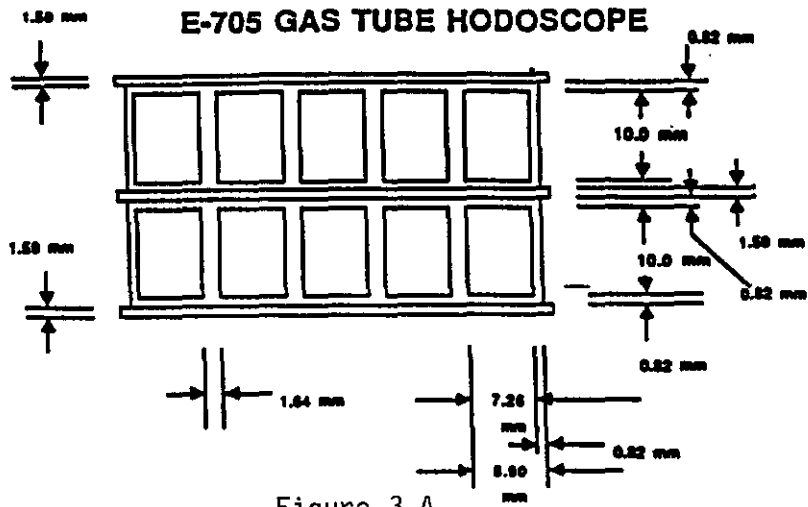


Figure 3 A

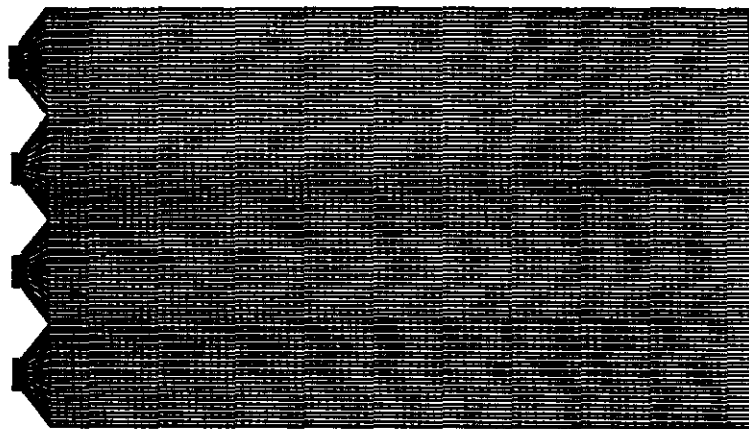


Figure 3B

#### SIDE VIEW E-705 GAS TUBE HODOSCOPE

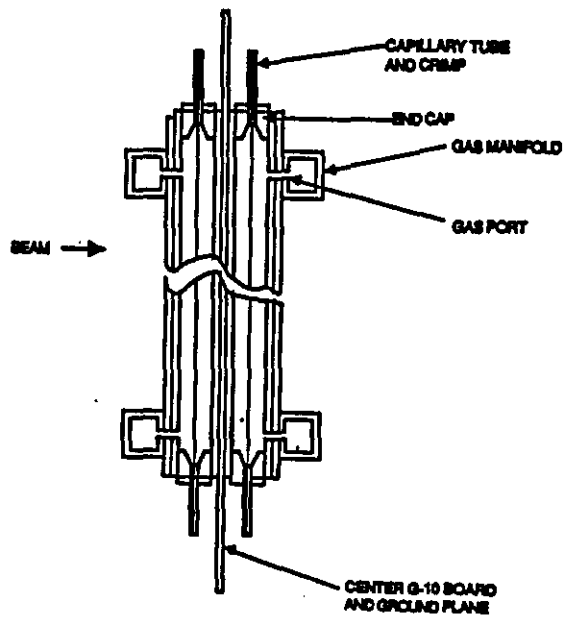
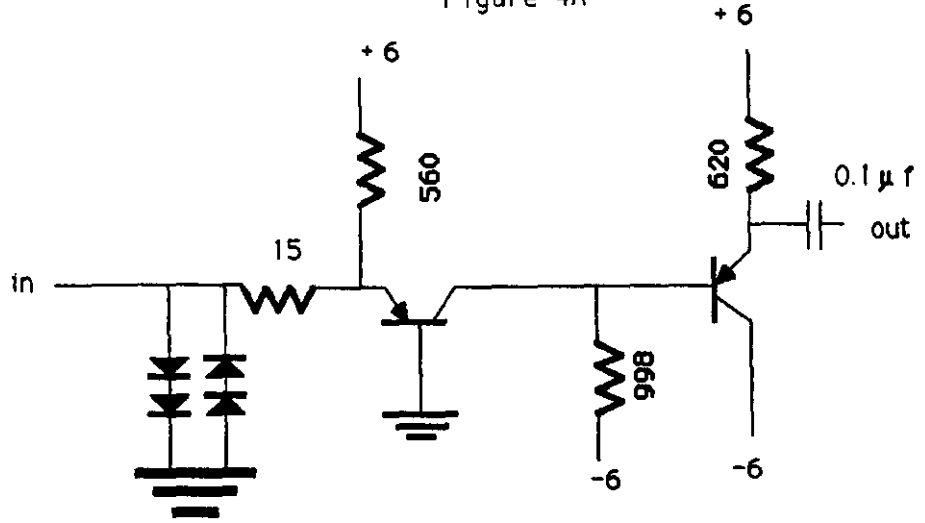


Figure 3C

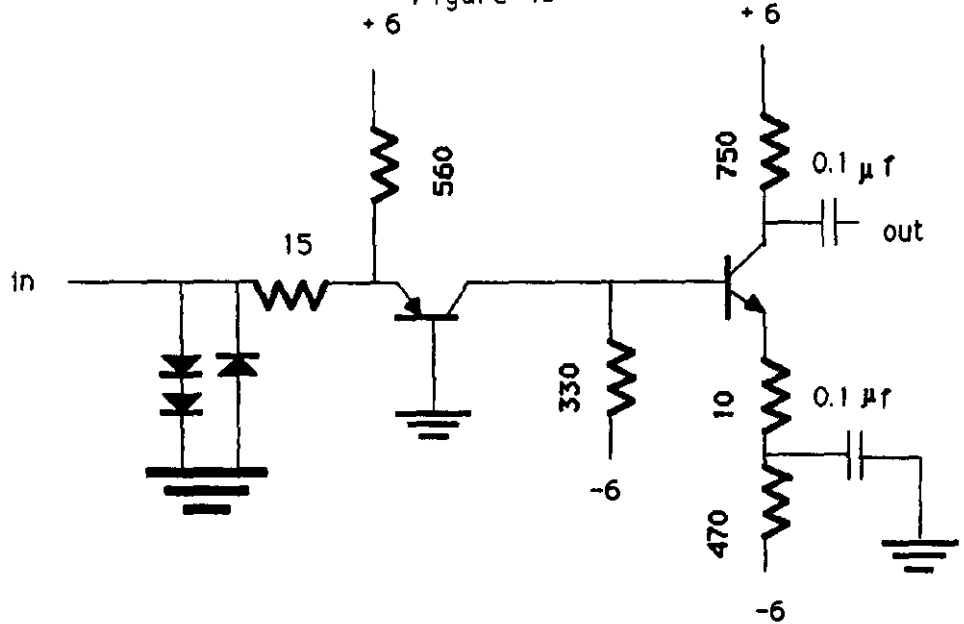
### ANODE AMPLIFIER

Figure 4A



### CATHODE AMPLIFIER

Figure 4B



### Test Chamber with Ru Source

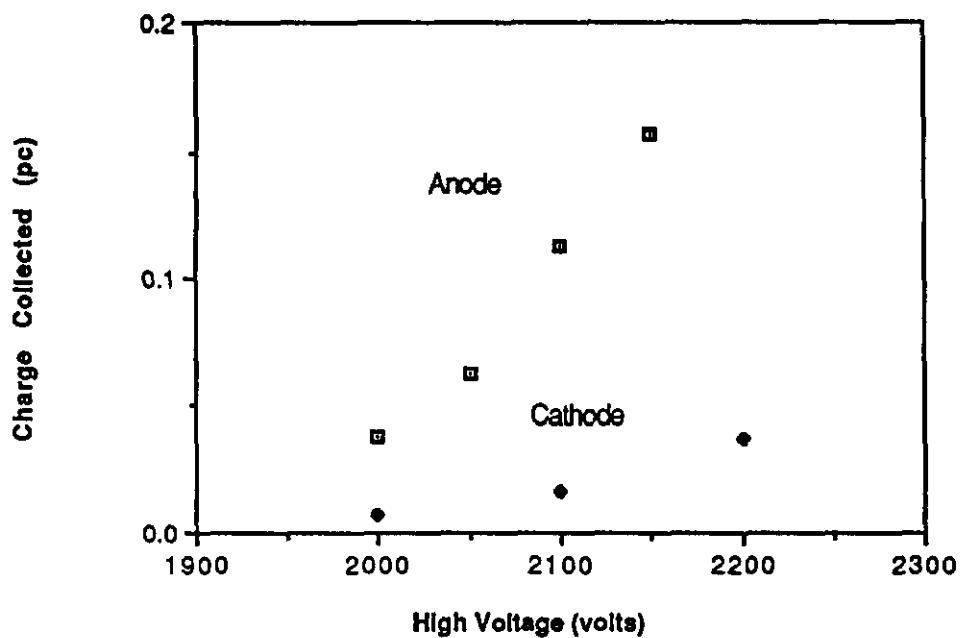


Figure 5

### CHARGE COLLECTED VS HIGH VOLTAGE

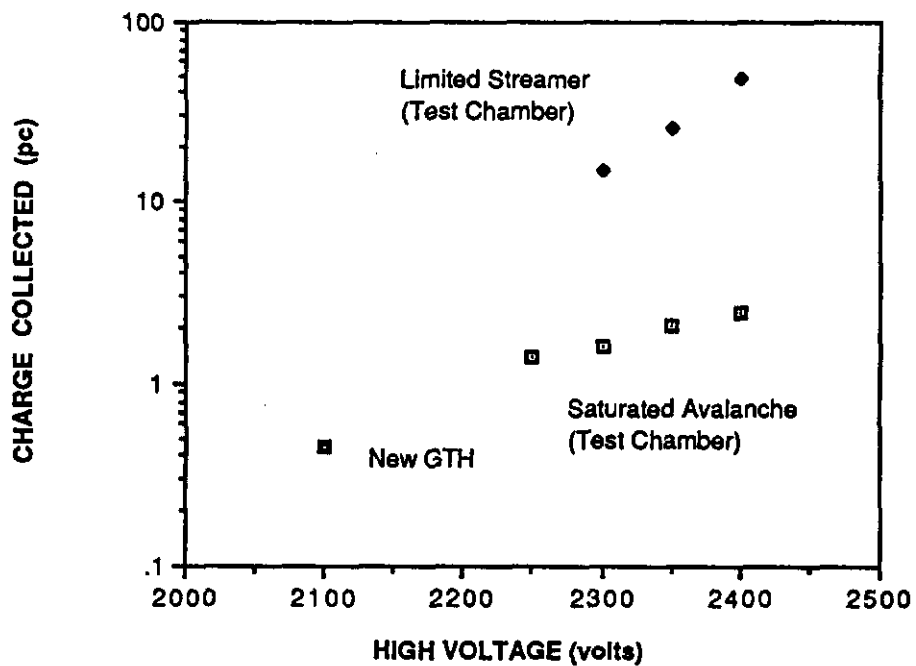
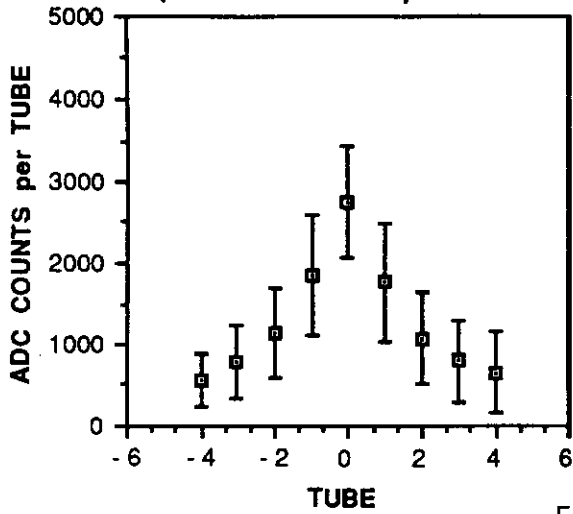


Figure 6

**Profiles 60 GeV Electron Showers  
(X Anode Wires)**



**Profiles 60 GeV Electron Showers  
(Y Cathode Strips)**

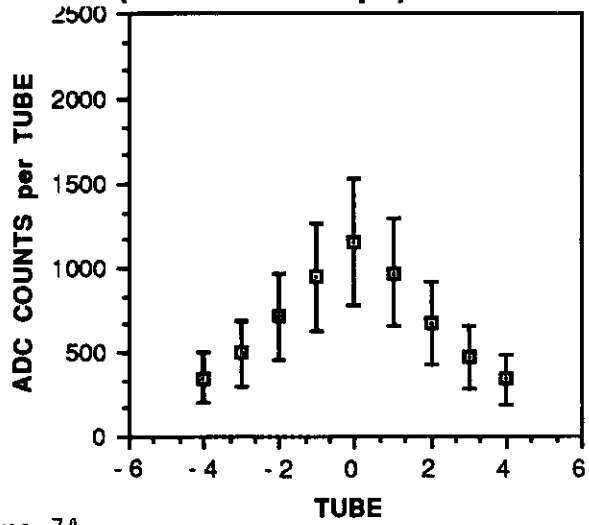
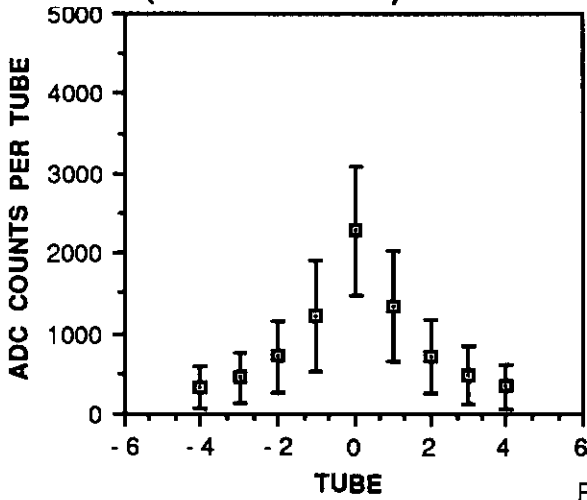


Figure 7A

**Profiles 30 GeV Electron Showers  
(X Anode Wires)**



**Profiles 30 GeV Electron Showers  
(Y Cathode Strips)**

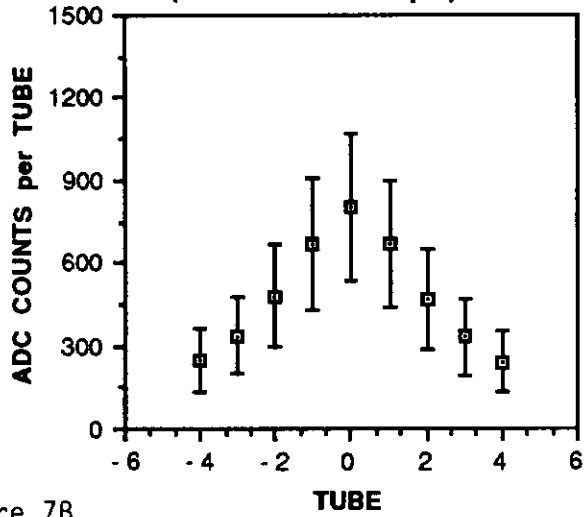
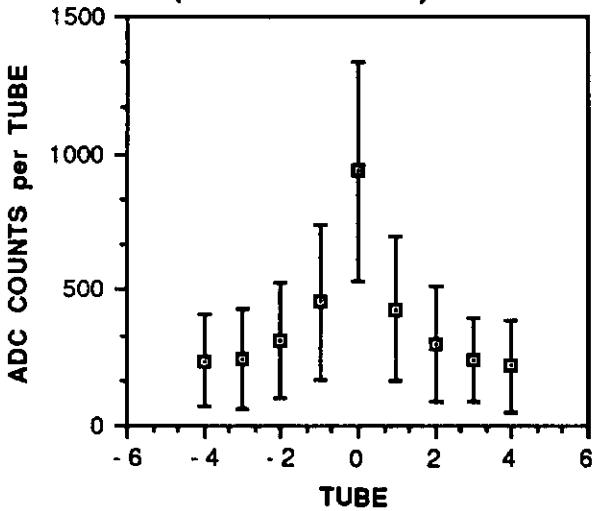


Figure 7B

**Profiles 6 GeV Electron Showers  
(X Anode Wires)**



**Profiles 6 GeV Electron Showers  
(Y Cathode Strips)**

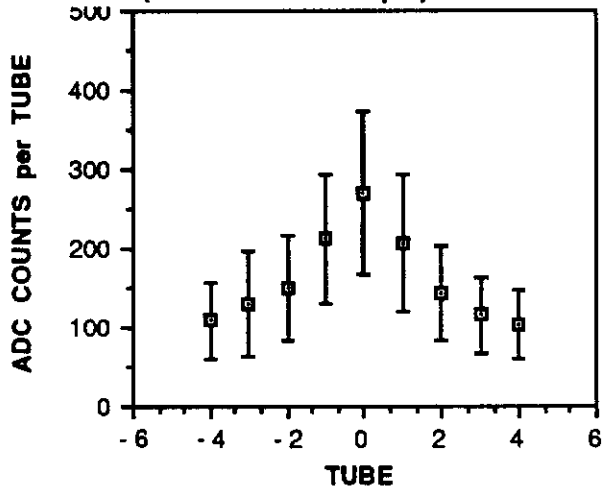


Figure 7C

**Total ADC Counts for Electrons  
(X Anode)**



Figure 8A

**Total ADC Counts for Electrons  
(Y Cathode Strips)**

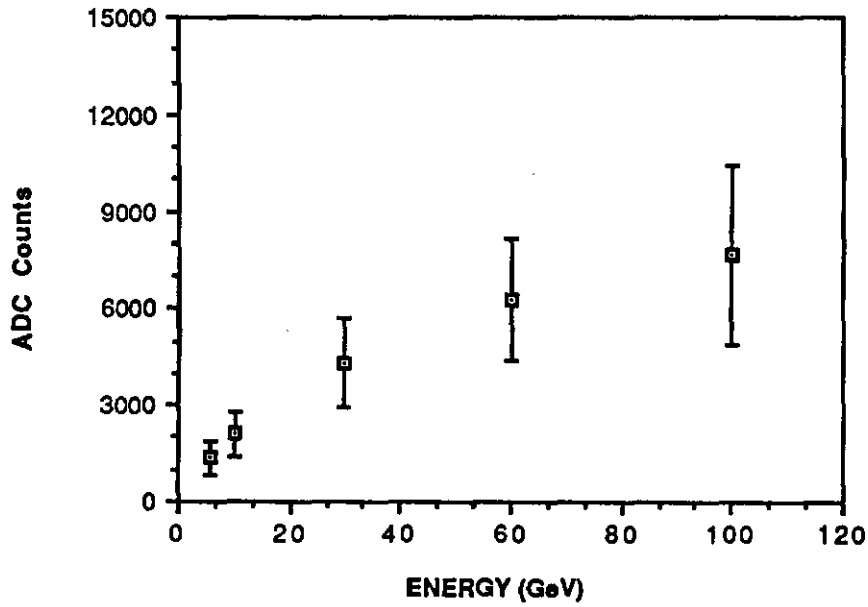


Figure 8B

Width of showers from fit

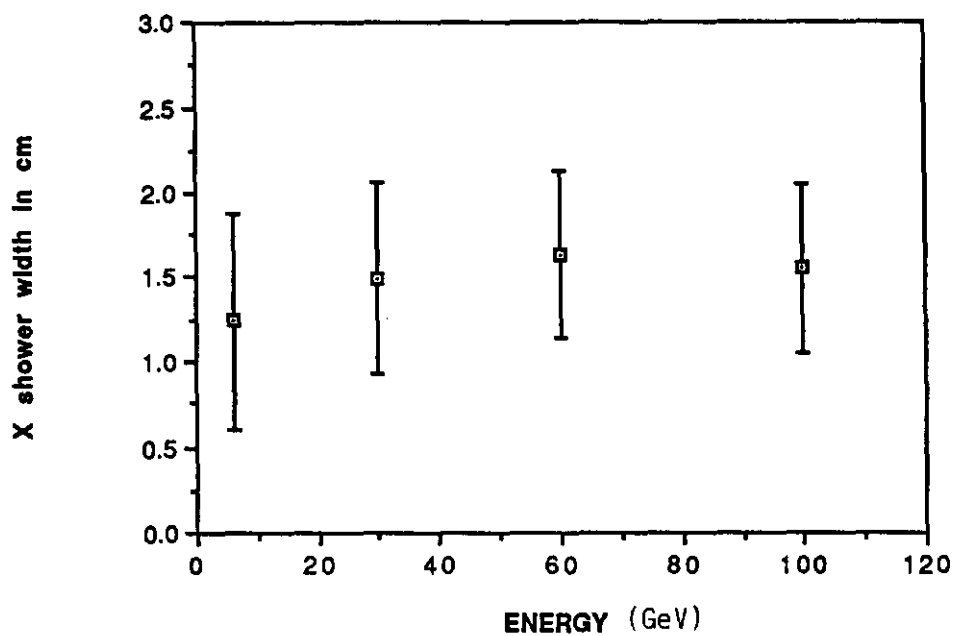


Figure 9A

Width of showers from fit

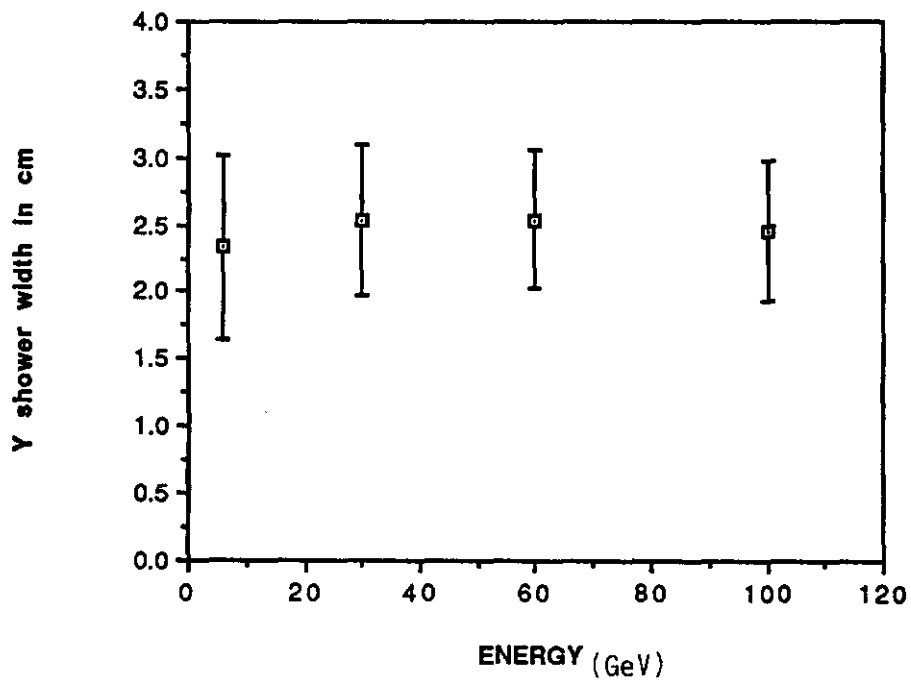


Figure 9B

### X anode Resolution GTH (beam error corrected)

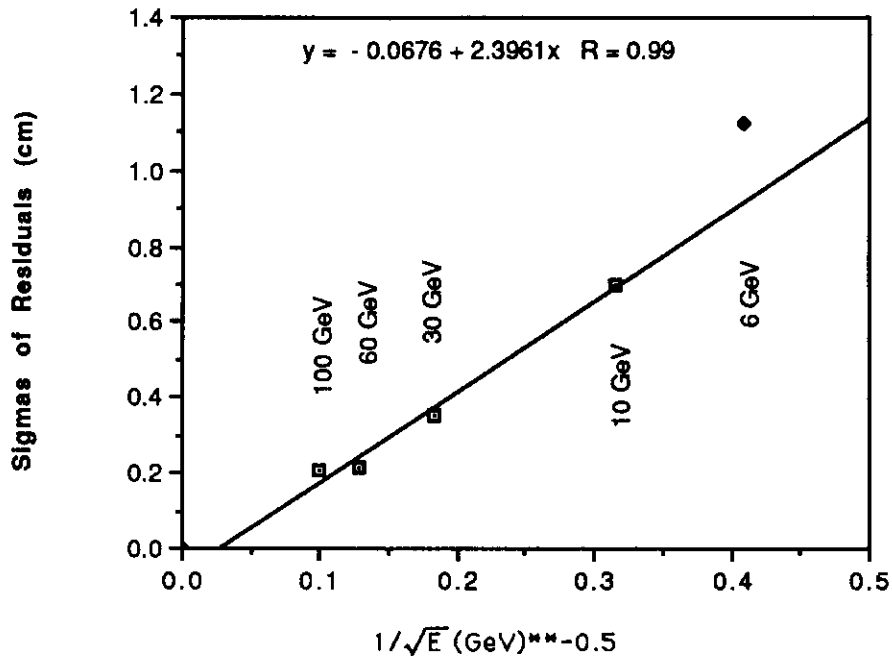


Figure 10 A

### Y cathode strip Resolution (beam error corrected)

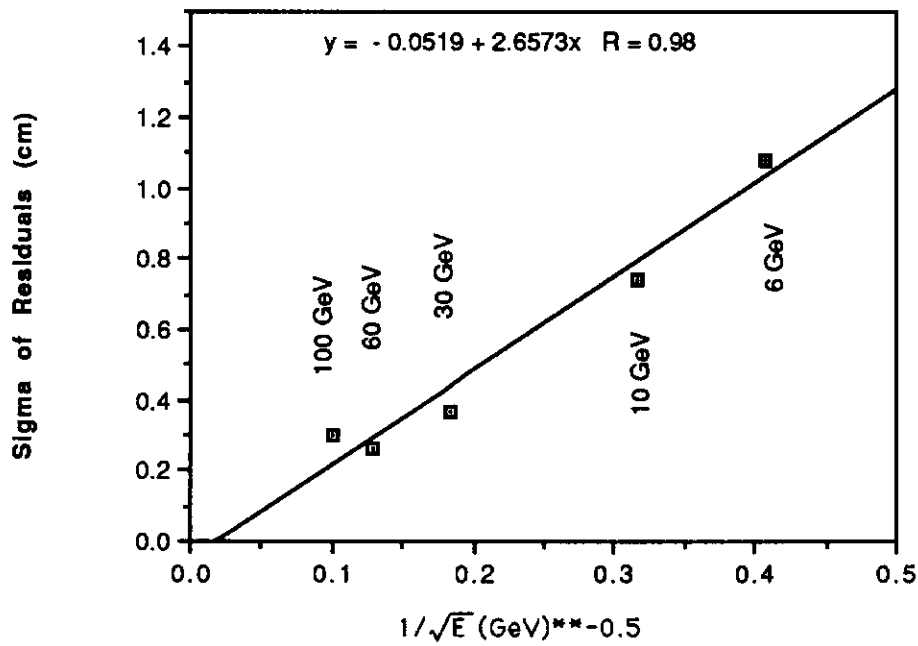


Figure 10 B